

## A Two-Dimensional DNA Array: The Three-Layer Logpile

Jonathan Malo, James C. Mitchell, and Andrew J. Turberfield\*

Clarendon Laboratory, Department of Physics, University of Oxford, Parks Road, Oxford OX1 3PU, U.K.

Received May 26, 2009; E-mail: a.turberfield@physics.ox.ac.uk

DNA self-assembly is capable of creating nanometer-scale polyhedra,<sup>1</sup> simple machines,<sup>2</sup> two-<sup>3</sup> and three-dimensional arrays,<sup>4</sup> periodic tubes,<sup>5</sup> and aperiodic DNA origami.<sup>6</sup> These DNA structures are designed to self-assemble through control of the oligonucleotide sequences of the component DNA strands.<sup>7</sup> Periodic DNA nanostructures have a specific application in structural biology as templates to create synthetic protein crystals,<sup>8</sup> including 2D protein crystals suitable for structure determination using cryo-electron microscopy.<sup>3h</sup> We present a 2D array, the three-layer logpile (3LL), which is designed to maximize structural order by ensuring that helices run continuously, without bending, through the structure.

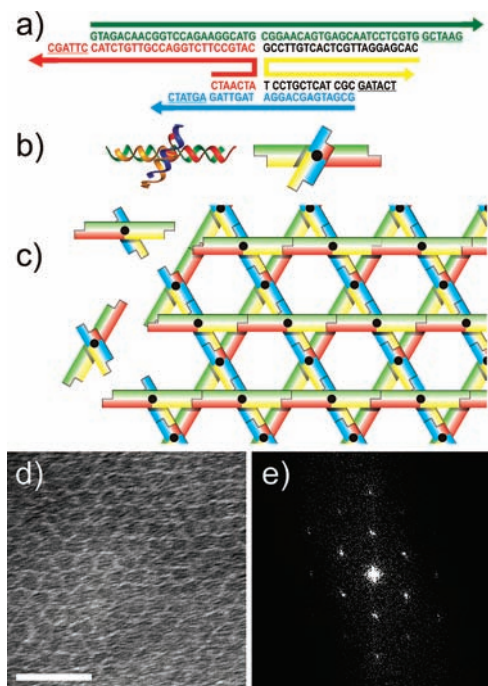


**Figure 1.** Three-layer logpile. (a) Basic structural unit: four oligonucleotides hybridize to form an immobile Holliday junction. Arrows indicate 5'–3' sequence polarity; unpaired nucleotides are underlined. (b) 3D representations of the junction showing the arrangement of sticky ends. (c) The 3LL lattice is formed by assembly of many Holliday junctions through hybridization of sticky ends. Dots indicate the positions of the junctions; at other points helices in the top and bottom layers cross without touching. (d) TEM image of the 3LL lattice. DNA is negatively stained so it appears light against a dark background. Scale bar: 50 nm. (e) Reciprocal space image of the 3LL lattice.

Compared to most previously reported 2D DNA arrays,<sup>3a–k</sup> the 3LL has a relatively small unit cell, ~15.6 nm, and is constructed from a simple motif. The basic building block consists of four oligonucleotides hybridized to form a single, immobile  $\chi$ -stacked Holliday junction<sup>9</sup> (Figure 1a,b). The Holliday junction has four double-stranded DNA arms, each of which terminates in a sticky end consisting of six unpaired bases. Since the red sticky end is

complementary to the green and the yellow sticky end is complementary to the blue, their hybridization results in the assembly of a two-dimensional array (Figure 1c). Each four-armed junction can be considered as two quasi-continuous duplexes connected by exchange of two strands where they meet: the duplexes are stacked on top of each other with a 60° right-handed twist between them.<sup>9</sup> One duplex is twice the length of the other. The two-dimensional array consists of three layers of helices, each running at 60° to the others. The shorter duplexes (2.5 DNA turns in length) join end-to-end to form the middle layer of helices, and the longer duplexes (5 DNA turns in length) form the top and bottom layers of the lattice. Only one layer (the middle layer) of helices is joined to both other layers. In contrast to the woven structure of the kagome lattice reported previously,<sup>3h</sup> the helices are designed to be straight, to avoid distortions that might reduce crystalline order.

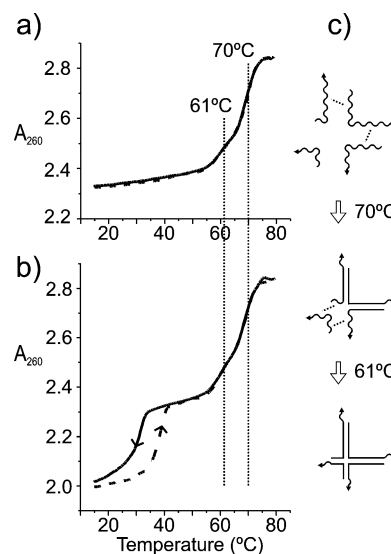


**Figure 2.** Temperature-controlled self-assembly of the 3LL array. Hybridization is associated with a decrease in absorbance at 260 nm ( $A_{260}$ ). (a) Control: Holliday junction assembly. A stoichiometric mixture of truncated 3LL oligonucleotides, lacking sticky ends, is cooled from above the melting temperature (solid lines), then remelted (dashed lines). (b) Assembly of the 3LL array from the full-length oligonucleotides. Hysteresis is associated with array formation. Concentration of each component: 1.5  $\mu\text{M}$ . Rate of change of temperature: 0.1  $^{\circ}\text{C min}^{-1}$ . Dotted lines indicate calculated transition temperatures corresponding to the assembly steps shown in (c).

Assembly of the 3LL can be followed by measuring the decrease in  $A_{260}$ , the absorbance at 260 nm, as a mixture of its component oligonucleotides is slowly cooled. ( $A_{260}$  decreases as oligonucleotides hybridize.) Figure 2 shows  $A_{260}$  as a function of temperature as stoichiometric mixtures of oligonucleotides are slowly annealed and then remelted. Figure 2a shows the formation of the 3LL junction from oligonucleotides lacking sticky ends such that assembly of the extended array cannot occur. Dotted lines in

and 61 °C mark calculated transition temperatures<sup>10</sup> which correspond to particular junction assembly steps (Figure 2c): first the three longest oligonucleotides hybridize to form the two long arms, and then the shortest strand hybridizes to complete junction formation. Cooling and melting curves are overlaid: no significant hysteresis is observed. Assembly and melting of the 3LL oligonucleotides with sticky ends is shown in Figure 2b. Although reversible assembly of the junction at high temperature is again observed, below ~42 °C there is rate-dependent hysteresis that we associate with the assembly of extended arrays of junctions by hybridization of sticky ends. This is consistent with the observation that slow cooling in the range 40–20 °C improves the size and crystalline order of the arrays, whereas slow cooling at higher temperatures does not.

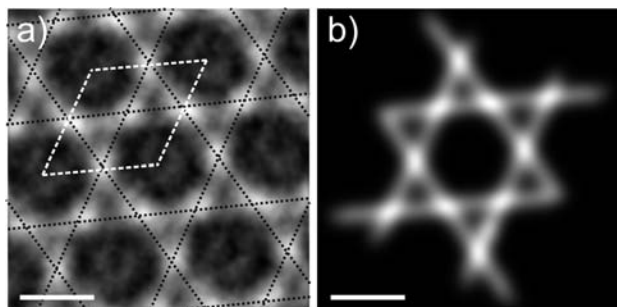


**Figure 3.** (a) Averaged image of a small region of 3LL lattice derived from a negatively stained TEM image. White dashed lines define the primitive unit cell of the lattice, which exhibits  $p1$  plane group symmetry ( $a, b = 15.6$  nm,  $\gamma = 120^\circ$ ). Black dotted lines indicate the positions of the helices. (b) 2D projection of a computer-generated model of the 3LL lattice, blurred to give a resolution of 2.0 nm. Scale bars: 10 nm.

Negative-stain transmission electron microscopy (TEM) of 3LL samples shows that the arrays form extensive sheets ( $\sim \mu\text{m}^2$ ) with a honeycomb appearance (Figure 1d) and an approximately hexagonal lattice (Figure 1e). Contrast between DNA and background is low, and the signal-to-noise ratio is limited by the need to use low electron-beam current densities to avoid damage. However, by combining image data from many unit cells we have been able to obtain higher resolution structural information.

Figure 3 shows an image of the 3LL array obtained by a process of iterative correlation mapping and averaging<sup>11a</sup> using SPIDER,<sup>11b</sup> a software package written for image processing of single-particle TEM images. The positions of right-handed junctions and left-handed nonjunction crossovers are indicated by ellipsoidal regions of high density. Nonjunction crossovers occur between helices in the top and bottom layers of the lattice (Figure 1c). The distance between crossovers is 7.8 nm, 1 nm shorter than the expected contour length of the DNA between them. This may be due to shrinkage of the DNA caused by dehydration during TEM grid preparation.<sup>12</sup>

Only a few 2D DNA lattice structures have been characterized with TEM,<sup>3b</sup> the majority having been investigated using atomic force microscopy (AFM). Our results for the 3LL, kagome lattice,<sup>3b</sup> and DNA tetrahedron<sup>1f</sup> show that TEM can provide high structural resolution: we estimate that the resolution of Figure 3 is between 3.0 and 3.5 nm. TEM is becoming an essential tool for DNA nanotechnology;<sup>1d–f</sup> further improvements in imaging resolution will be coupled to improvements in the structural order and homogeneity of the self-assembled nanostructures.

**Acknowledgment.** We thank Dr. Jonathan Bath and Anthony Walsh (Oxford Physics) for experimental assistance and the Oxford Materials Department for providing access to electron microscopy facilities. This work was supported by the MoD and by the UK research councils BBSRC, EPSRC, and MRC through the UK Bionanotechnology IRC.

**Supporting Information Available:** DNA sequences, supplementary methods, characterization of junction assembly, micrographs of extended arrays. This material is available free of charge via the Internet at <http://pubs.acs.org>.

## References

- (1) (a) Chen, J. H.; Seeman, N. C. *Nature* **1991**, *350*, 631–633. (b) Zhang, Y. W.; Seeman, N. C. *J. Am. Chem. Soc.* **1994**, *116*, 1661–1669. (c) Goodman, R. P.; Schaap, I. A. T.; Tardin, C. F.; Erben, C. M.; Berry, R. M.; Schmidt, C. F.; Turberfield, A. J. *Science* **2005**, *310*, 1661–1665. (d) Shih, W. M.; Quispe, J. D.; Joyce, G. F. *Nature* **2004**, *427*, 618–621. (e) He, Y.; Ye, T.; Su, M.; Zhang, C.; Ribbe, A. E.; Jiang, W.; Mao, C. D. *Nature* **2008**, *452*, 198–201. (f) Kato, T.; Goodman, R. P.; Erben, C. M.; Turberfield, A. J.; Namba, K. *Nano Lett.* **2009**, *9*, 2747–2750.
- (2) (a) Mao, C.; Sun, W.; Shen, Z.; Seeman, N. C. *Nature* **1999**, *397*, 144–146. (b) Yurke, B.; Turberfield, A. J.; Mills, A. P.; Simmel, F. C.; Neumann, J. L. *Nature* **2000**, *406*, 605–608. (c) Liao, S. P.; Seeman, N. C. *Science* **2004**, *306*, 2072–2074. (d) Shin, J.-S.; Pierce, N. A. *J. Am. Chem. Soc.* **2004**, *126*, 10834–10835. (e) Sherman, W. B.; Seeman, N. C. *Nano Lett.* **2004**, *4*, 1203–1207. (f) Yin, P.; Yan, H.; Danielli, X. G.; Turberfield, A. J.; Reif, J. H. *Angew. Chem., Int. Ed.* **2004**, *43*, 4906–4911. (g) Tian, Y.; He, Y.; Peng, Y.; Mao, C. *Angew. Chem., Int. Ed.* **2005**, *44*, 4355–4358. (h) Bath, J.; Green, S. J.; Turberfield, A. J. *Angew. Chem., Int. Ed.* **2005**, *44*, 4358–4361. (i) Green, S. J.; Bath, J.; Turberfield, A. J. *Phys. Rev. Lett.* **2008**, *101*, 238101.
- (3) (a) Winfree, E.; Liu, F.; Wenzler, L. A.; Seeman, N. C. *Nature* **1998**, *394*, 539–544. (b) Mao, C. D.; Sun, W. Q.; Seeman, N. C. *J. Am. Chem. Soc.* **1999**, *121*, 5437–5443. (c) LaBean, T. H.; Yan, H.; Kopatsch, J.; Liu, F. R.; Winfree, E.; Reif, J. H.; Seeman, N. C. *J. Am. Chem. Soc.* **2000**, *122*, 1848–1860. (d) Yan, H.; Park, S. H.; Finkelstein, G.; Reif, J. H.; LaBean, T. H. *Science* **2003**, *301*, 1882–1884. (e) Liu, D.; Wang, M.; Deng, Z.; Walulu, R.; Mao, C. J. *Am. Chem. Soc.* **2004**, *126*, 2324–2325. (f) Ding, B.; Sha, R.; Seeman, N. C. *J. Am. Chem. Soc.* **2004**, *126*, 10230–10231. (g) Chelyapov, N.; Brun, Y.; Gopalkrishnan, M.; Reishus, D.; Shaw, B.; Adleman, L. *J. Am. Chem. Soc.* **2004**, *126*, 13924–13925. (h) Malo, J.; Mitchell, J. C.; Vénien-Bryan, C.; Harris, J. R.; Wille, H.; Sherratt, D. J.; Turberfield, A. J. *Angew. Chem., Int. Ed.* **2005**, *44*, 3057–3061. (i) Mathieu, F.; Liao, S.; Kopatsch, J.; Wang, T.; Mao, C.; Seeman, N. C. *Nano Lett.* **2005**, *5*, 661–665. (j) He, Y.; Chen, Y.; Liu, H.; Ribbe, A. E.; Mao, C. *J. Am. Chem. Soc.* **2005**, *127*, 12202–12203. (k) He, Y.; Tian, Y.; Ribbe, A. E.; Mao, C. *J. Am. Chem. Soc.* **2006**, *128*, 15978–15979. (l) Zhang, C.; He, Y.; Chen, Y.; Ribbe, A. E.; Mao, C. *J. Am. Chem. Soc.* **2007**, *129*, 14134–14135.
- (4) (a) Paukstelis, P. J.; Nowakowski, J.; Birktoft, J. J.; Seeman, N. C. *Chem. Biol.* **2004**, *11*, 1119–1126. (b) Nykypanchuk, D.; Maye, M. M.; van der Lelie, D.; Gang, O. *Nature* **2008**, *451*, 549–552. (c) Park, S. Y.; Lytton-Jean, A. K. R.; Lee, B.; Weigand, S.; Schatz, G. C.; Mirkin, C. A. *Nature* **2008**, *451*, 553–556.
- (5) (a) Mitchell, J. C.; Harris, J. R.; Malo, J.; Bath, J.; Turberfield, A. J. *J. Am. Chem. Soc.* **2004**, *126*, 16342–16343. (b) Rothmund, P. W. K.; Ekani-Nkodo, A.; Papadakis, N.; Kumar, A.; Fyngenson, D. K.; Winfree, E. *J. Am. Chem. Soc.* **2004**, *126*, 16344–16352. (c) Ke, Y. G.; Liu, Y.; Zhang, J. P.; Yan, H. *J. Am. Chem. Soc.* **2006**, *128*, 4414–4421.
- (6) Rothmund, P. W. K. *Nature* **2006**, *440*, 297–302.
- (7) (a) Seeman, N. C. *J. Biomol. Struct. Dyn.* **1990**, *8*, 573–581. (b) Dirks, R. M.; Lin, M.; Winfree, E.; Pierce, N. A. *Nucleic Acids Res.* **2004**, *32*, 1392–1403. (c) Goodman, R. P. *Biotechniques* **2005**, *38*, 548–550.
- (8) Seeman, N. C. *J. Theor. Biol.* **1982**, *99*, 237–247.
- (9) Ortiz-Lombardia, M.; Gonzalez, A.; Eritja, R.; Aymami, J.; Azorin, F.; Coll, M. *Nat. Struct. Biol.* **1999**, *6*, 913–917.
- (10) (a) Peyret, N.; Seneviratne, P. A.; Allawi, H. T.; SantaLucia, J. *Biochemistry* **1999**, *38*, 3468–3477. (b) SantaLucia, J. *Proc. Natl. Acad. Sci. U.S.A.* **1998**, *95*, 1460–1465.
- (11) (a) Wille, H.; Michelitsch, M. D.; Guénebaud, V.; Supattapone, S.; Serban, A.; Cohen, F. E.; Agard, D. A.; Prusiner, S. B. *Proc. Natl. Acad. Sci. U.S.A.* **2002**, *99*, 3563–3568. (b) Frank, J.; Radermacher, M.; Penczek, P.; Zhu, J.; Li, Y.; Ladjadj, M.; Leith, A. *J. Struct. Biol.* **1996**, *116*, 190–199.
- (12) (a) Vollenweider, H. J.; James, A.; Szybalski, W. *Proc. Natl. Acad. Sci. U.S.A.* **1978**, *75*, 710–714. (b) Lee, G.; Arscott, P. G.; Bloomfield, V. A.; Evans, D. F. *Science* **1989**, *244*, 475–477.

JA9042593